

FIELDS AND SURFACE IRREGULARITY FACTORS OF STRANDED CONDUCTORS IN CO-AXIAL CYLINDER CONFIGURATIONS

Mahmoud Mohamed EL-Bahy

Faculty of Engineering, Benha University, Cairo, Egypt

(Received April 30, 2007 Accepted, May 21, 2007)

This paper aims to investigate theoretically the electric fields and the surface irregularity factors for stranded conductors in pressurized air and SF₆ in co-axial cylinder configurations. The surface irregularity factor is defined as the ratio of the corona onset voltage of a stranded conductor to that of a smooth cylindrical conductor of the same outer diameter. This calls for the assessment of the electric field in the vicinity of the stressed conductor and the corona onset voltage. The investigated gap is a three dimensional field problem. To solve this problem, charge simulation technique (CST) is used, where the simulation charges for stressed and grounded conductors are helical of infinite length. The method of corona onset voltage calculation is based on the criterion developed for the formation of repetitive negative corona Trichel pulses. The effects of varying conductor radius, gas pressure, stranding ratio on the irregularity factor values are investigated. The calculated values of irregularity factor in air agree well with those calculated and measured before.

1. INTRODUCTION

For the transmission of high power over long distances, gas-insulated transmission lines (GITL) in addition to cables are suitable alternatives to overhead lines in heavily populated areas. Gas-insulated transmission lines (GITL) are used since more than 30 years for linking power plants to the transmission network as well as for links within gas-insulated substations (GIS) [1]. Alternating current (ac) SF₆ GITL of ratings up to 800 kV, 8 kA, 4GVA and 100 km are in service for high-power and long distance transmission [1, 2]. Direct current (dc) transmission serves a dual purpose, that is: interconnection of systems especially those operated at different frequencies, and for long-distance bulk energy transfer. DC GIS of rating 500 kV has been developed [3].

Practical transmission lines are normally of stranded construction and often contain surface irregularities. Stranded conductors are composed of 7, 19, 37,...etc strands in continuing fixed increments and the external layer twists around interior layers in helical form. Conductors are stranded mainly to increase their flexibility with a subsequent increase of the mechanical strength. Stranding distorts the electric field in the immediate vicinity of the conductor and reduces the surface irregularity factor, m [4, 5]. The influence of stranding was characterized by introducing a surface irregularity factor m [6 - 8]. The value of m equals unity for a perfectly smooth conductor, and is less than 1 for stranded conductors.

This paper aims to investigate theoretically the electric fields and the surface irregularity factors for stranded conductors in pressurized air and SF₆ in co-axial cylinder configurations. This calls for the assessment of the electric field in the vicinity of the stressed conductor and the corona onset voltage. The investigated gap is a three dimensional field problem. The accurate CST is used for field calculation in the vicinity of the stressed conductors. The simulating charges for both the stressed conductor and the grounded cylinder take the helical form. The onset voltage calculation is based on the criterion developed for the formation of repetitive negative corona Trichel pulses. The effects of varying the conductor radius, gas pressure and stranding ratio on the irregularity factors are investigated. The calculated values of irregularity factors in air agree satisfactorily with those values obtained before theoretically [5] and experimentally [8].

2. TWISTING OF EXTERNAL LAYER OF STRANDED CONDUCTOR

The outer layer of stranded conductors twists around the inner layers in a helical form. The locus of a point which moves in a uniform motion along a generatrix around circular conductor is called a helix [9]. The length of one complete revolution of this point around the conductor axis is called a pitch and it is repeated along the helix. Practically, the pitch length (L_p) equals the pitch factor (PF) times the overall diameter ($2R$) of the conductor [10] and PF for 7, 19 and 37 stranded conductors equals 16-18, 14-16 and 12-14, respectively [10]. Hence, $L_p = 2R \times PF$, where, PF is chosen to be 17, 15 and 13 for 7, 19 and 37 stranded conductors, respectively. The location of this point is related to pitch length (L_p) and the conductor radius (R).

3. METHOD OF ANALYSIS

3.1. Electric Field Calculation around Stranded Conductor

The analysis is based on CST in which the distributed charges on the surface of the stressed conductor are replaced by a set of fictitious simulation charges arranged inside the external layer of stranded conductors. The number of charges is 3 times the number of strands n_o of the outer layer. Also, the distributed charge on the surface of the outer (grounded) cylinder is simulated by another set of n_g helical charges uniformly distributed around it. Each helical charge is divided into infinite number of pitches where each pitch is subdivided into n finite line charges as shown in figure 1. The coordinates of simulating finite line charges and the coordinates of boundary points are chosen as described before [4], figure 2. Satisfaction of the Dirichlet boundary condition results in a set of equations whose simultaneous solution determines the unknown simulation charges [4]. With the knowledge of simulation, charges, the electric field can be calculated at conductor surface and its near vicinity as explained in appendix A.

3.2. Surface Irregularity Factor Calculation

To calculate the surface irregularity factor, m , the onset voltage of corona is first calculated for stranded and smooth cylindrical conductors. The method of corona onset calculation is explained clearly before [4, 11]. Onset voltage calculations are obtained by using the available physical parameters of air and SF₆ [12].

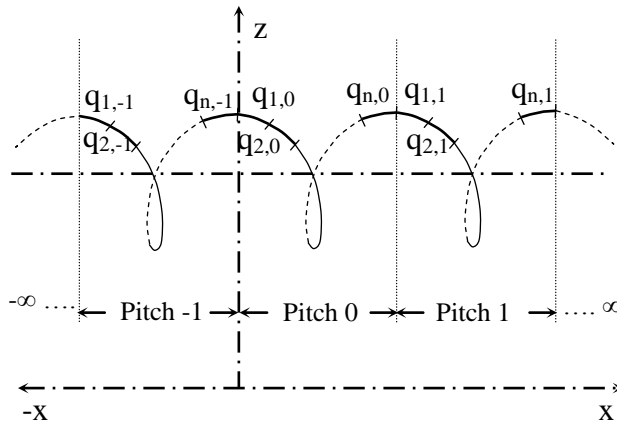


Figure 1: Division of the helical charge, q_h , into infinite number of pitches ($-\infty, \dots, -k, \dots, -1, 0, 1, \dots, k, \dots, \infty$) and division of that charge in each pitch into n finite line charges.

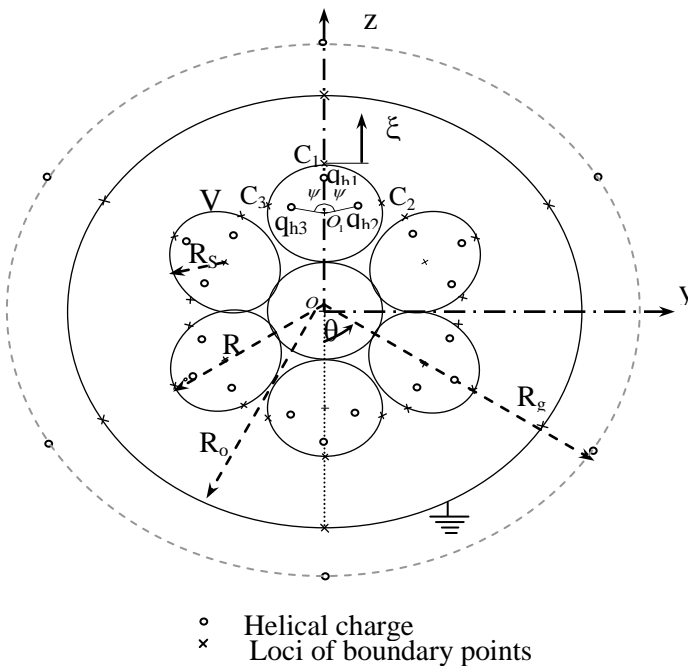


Figure 2: The location of helical charges and boundary points loci in cross section of 7 stranded conductor placed at the center of an outer (grounded) cylinder.

4. RESULTS AND DISCUSSION

To check the accuracy of the charge simulation, check points are selected over the conductor and outer cylinder circumferences. Each point lies midway between two successive boundary points on the same locus. The potential and the deviation angle of the field are assessed at the check points to check how well the boundary condition is satisfied. This check was made for stranded conductors' radii of 1 and 25 mm. The accuracy remained the same for this investigated range as given for samples computed at outer cylinder radius $R_o = 1m$.

The accuracy of a simulation depends strongly on the assumptions concerned with the choice of the number and coordinates of the simulation charges. In pitch-0, the number of the finite line charges was assumed to be $N = n \times (3n_o + n_g)$. The best values of n_g and n were found to be 6 and 40, respectively. Hence, $N = 960, 1680$ and 2400 for 7, 19 and 37 stranded conductors, respectively. The effective number of pitches $(I+2k)$ for these stranded conductors was found to depend on the radius of the outer conductor R_o , wherever the best value of k was found to be integer of $(80 R_o + 12)$, i. e. for $R_o = 1 m$, k will be 92 pitch. As a result the effective length achieving the simulation accuracy of the stranded conductor will be equal to $[I+2 \times (80 R_o + 12)] \times 2R \times PF$. It depends on the radius of the outer and inner conductor radii and type of stranding.

At the circumference of check points, the percentage errors of the potential and the electric field deviation angle in y-z plane are calculated. Figure 3 shows the percentage errors of the calculated potential for 7, 19 and 37 stranded conductors. The maximum per cent error does not exceed 0.1%. At the surface of the outer cylinder the per cent potential error does not exceed 1.5×10^{-3} %. Potential errors on the conductor surface of less than 0.1 % are considered reasonable for accurate field solution [13]. Over most of the stranded conductor surfaces, (except narrow zones that lie near the contact points of the outer layer strands), the electric field deviation angle does not exceed 3.2, 2.6 and 2.7 degrees for 7, 19 and 37 stranded conductors, respectively. As given in [4], the field values near the contact points of the outer layer strands is very low around the conductor circumference, hence, the error in the field deviation angle in y-z plane near these points has no effect on the onset voltage of corona.

Figure 4 gives the normalized electric field distributions near stressed stranded conductors with different values of n_o . It is defined as the ratio of the electric field of a stranded conductor to that of a smooth cylindrical conductor, (E_{pu}). Two properties of these distributions should be noted. First, the maximum values of the normalized surface electric field for $n_o = 6, 12$ and 18 strands, equal 1.413, 1.438 and 1.45, respectively. For the same radius and gap length, similar values of (1.415, 1.430 and 1.441) and (1.407, 1.436 and 1.445) were theoretically obtained before using CST [4] and conformal mapping [14], respectively. These values indicate that the surface field is nearly independent of n_o and is in agreement with previous investigators [5, 15] who assigned 1.4 for the value of E_{pu} at the conductor surface, i.e. independent of n_o . Second, the larger n_o , the smaller is the region over which the electric field deviates from that of a smooth conductor, that region approaches zero as $n_o \rightarrow \infty$. Hence, the corona onset voltage for $n_o = 18$ is greater than both onset voltage values for $n_o = 6$ and 12 and approaches that of a smooth cylindrical conductor. This means that the surface irregularity factor m approaches unity as $n_o \rightarrow \infty$.

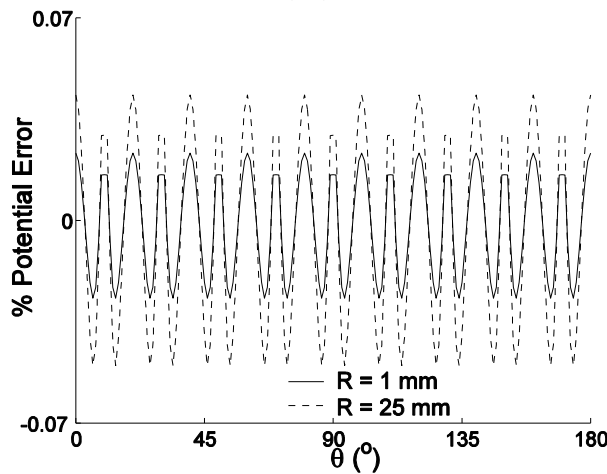
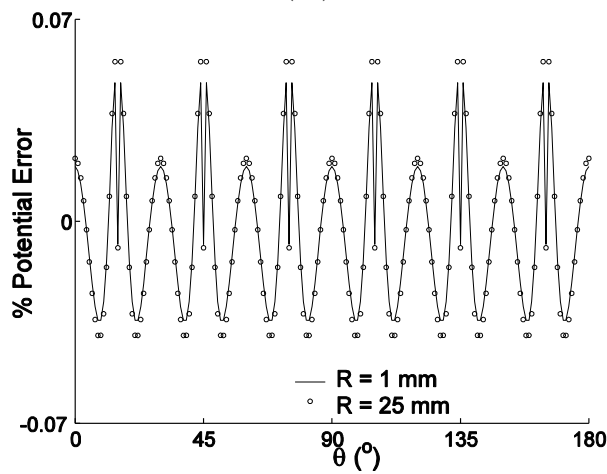
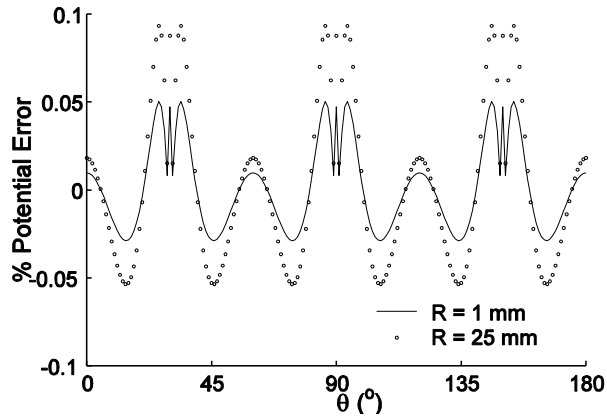


Figure 3: The variation of per cent potential errors at the check points around the circumferences of 7, 19 and 39 stranded conductors, respectively.

Figure 5 shows the calculated onset voltage against pressure for 37-stranded conductor having conductor radius $R = 10$ mm and extending along the axis of an outer cylinder of radius $R_o = 0.1$ m. The onset voltage values are calculated in SF_6 at the practical range of GITL pressure. To insulate the gap by air instead of SF_6 , the corresponding air pressure is obtained at the same onset voltage of corona from figure 5 and table 1.

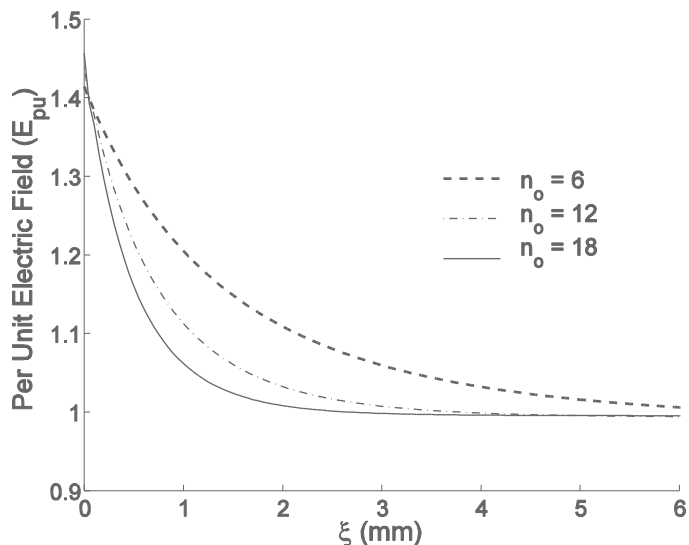


Figure 4: Normalized electric field distribution for 7, 19 and 37 stranded conductors, $R = 10$ mm and $R_o = 1$ m.

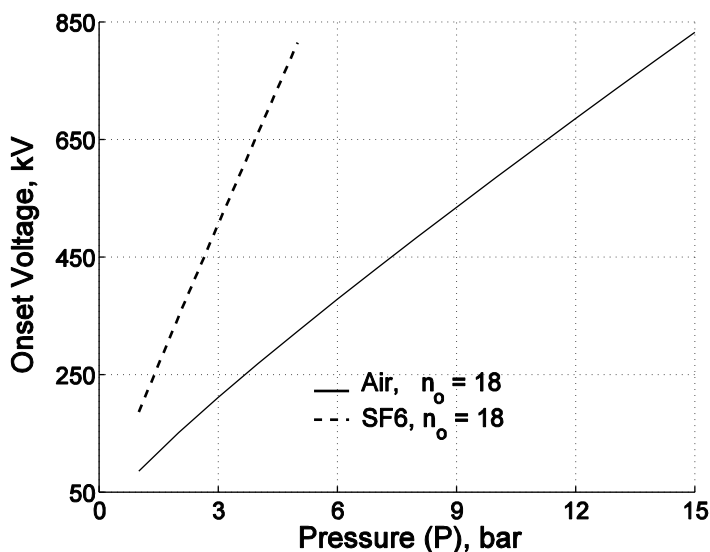


Figure 5: Onset voltage of corona on 37- stranded conductor against pressure at $R = 10$ mm and $R_o = 0.1$ m in SF_6 and air.

Table 1: The corresponding SF₆ and air pressures at the same onset voltage of corona for 37 stranded conductor, R = 10 mm and R_o = 0.1 m.

Onset voltage (kV)	186	348	506	661	814
SF ₆ pressure (bar)	1	2	3	4	5
Air pressure (bar)	2.58	5.44	8.43	11.50	14.62

Figure 6 shows the results for the surface irregularity factor *m* as a function of the stranding ratio ($= R_s / R$); this ratio equals 0.333, 0.2 and 0.143 for 7, 19 and 39 stranded conductors, respectively. As given in [5], the outer cylinder radius *R_o* was set to large enough value that it did not influence the results (*R_o* = 1 m). A comparison was made between data generated in the present study and Stone's data obtained by careful laboratory experimentation using specially manufactured stranded conductor having stranding ratios of 0.1 to 0.25 and conductor radius of 9.5 mm to 22.25 mm. These data seem to be the most credible experimental data available [8]. The irregularity factor obtained approaches unity with decreasing stranding ratio and hence is consistent with Stone's experimental data and the calculations provided by Yamazaki, and Olsen [5]. Further, the values are reasonably close to Stone's experimental data. In addition, the irregularity factor *m* increased slightly with a decrease of the stranded conductor radius *R* although this effect is smaller than that of the stranding ratio. That is because of its approach to the smooth conductor. It is also consistent with Stone's experimental data. Further, the values are reasonably close to the calculations provided by Yamazaki, and Olsen; with maximum difference of (2.6 %) due to the different onset voltage criteria. Yamazaki, and Olsen considered that corona is initiated at the critical avalanche size of 0.35×10^4 . In the present work the method of calculation is based on the criterion developed for the formation of repetitive negative corona Trichel pulses; (the avalanche size depends on the degree of nonuniformity, it varies from 0.30×10^4 to 80×10^4).

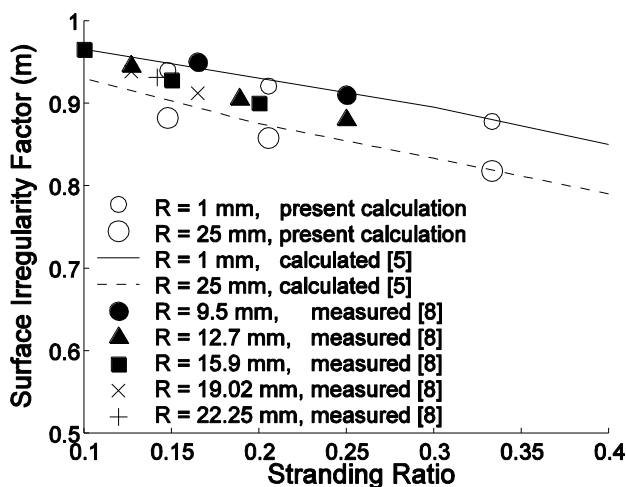
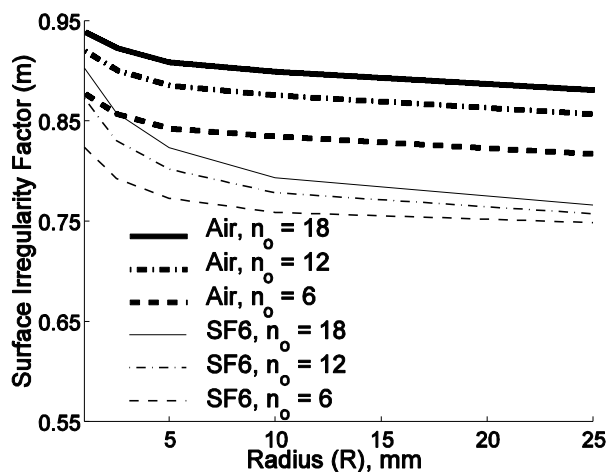
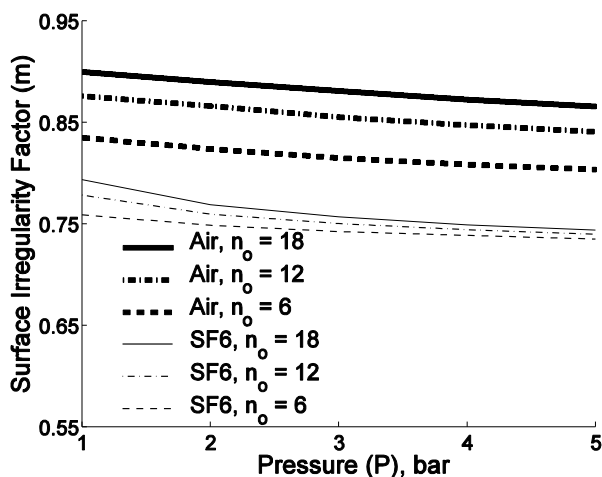


Figure 6: Surface irregularity factor *m* in air as a function of the stranding ratio *R_s/R*.

Figure 7 shows the results for the surface irregularity factor m for stranded conductors as a function of the conductor radius and the pressure of air and SF₆. As it is expected, the calculated surface irregularity factor m decreases with increasing the conductor radius, the stranding ratio and the gas pressure. Also, the calculated values of this factor in SF₆ is less than those calculated values in air as a result of severe reduction of SF₆ dielectric strength in the presence of conductor surface roughness [16].



(a)



(b)

Figure 7: Surface irregularity factor m in air and SF₆ for 7, 19 and 37 stranded conductors at outer cylinder radius $R_o = 1$ m as a function of the conductor radius R , at pressure = 1 bar (a) and the pressure (P) at conductor radius $R = 1$ mm (b).

5. CONCLUSIONS

1. Electric field distribution in the vicinity of stranded conductors in a coaxial cylinder configuration is a three-dimensional field problem. The electric field is calculated using charge simulation technique, where, both of the stressed and the grounded conductors are simulated by two sets of helical charges.
2. To achieve good accuracy, it was found that: the effective number of pitches depends on the outer conductor radius but it doesn't depend on the stressed conductor radius and type of stranding.
3. The accuracy of simulation is satisfied; the potential and the field deviation angle errors don't exceed 0.1% and 3.2 degrees over the effective conductor surface, respectively.
4. The maximum values of the surface electric field for stranded conductors divided by the maximum value of a smooth cylindrical conductor having the same radius are nearly independent of the number of strands n_o in the outer layer and equal approximately 1.4. This value agrees well with the values reported in the literature.
5. The calculated surface irregularity factor m was in good agreement with experimental data and theoretical values obtained before. It varies with stranding ratio, conductor radius, gas pressure and kind of insulating gas.

REFERENCES

1. O. Volker and H. Koch, "Insulation Co-ordination for gas-insulated Transmission lines (GIL)", IEEE Transactions on Power Delivery, Vol.16, No. 1, January 2001.
2. CIGRE Working Group 23/21/33.15, "Gas insulated lines (GIL)", Electra (206) pp.55-57, 2003.
3. T. Hasagawa, K. Yamaji, M. Hatano, F. Endo, T. Rokunohe, T. Yamagiwa, "Development of insulation structure and enhancement of insulation reliability of 500 kV dc GIS ", IEEE Transactions on Power Delivery, Vol.12-PWRD No. 1, pp. 194-202, 1997.
4. M. M. El-Bahy, M. Abouelsaad, N. Abdel-Gawad and M. Badawi, "Onset voltage of negative corona on stranded conductors", Journal of Physics D: Applied Physics, Vol. 40, No. 10, pp. 3094-3101, May 2007.
5. K. Yamazaki, and R. G. Olsen, " Application of a corona onset criterion to calculation of corona onset voltage of stranded conductors ", IEEE Transactions on Dielectrics and Electrical Insulation, Vol. 11, No. 4, pp. 674-680, August 2004.
6. F.W. Peek, "*Dielectric Phenomena in High Voltage Engineering*", Mc-Graw-Hill, New York, 1929.
7. J.B. Whitehead, "The electric strength of air, II ", AIEE Trans., Vol. 28, Pt. III, pp.1857-1887, 1911.

8. L.N. Stone, "EHV single and twin bundle conductors: influence of conductor diameter and strand diameter on radio influence voltage and corona initiation voltage", AIEE Transactions, Vol. 78, Part III, pp. 1434-1443, 1959.
9. M. Vygodsky, "Mathematical Handbook-Higher Mathematics", Mir Publishers, Moscow, 1971.
10. EL-Sewedy Industries, "Egytech Cables", Cairo, Egypt, 2006.
11. Mohamed Badawi Sayed Ahmed, "Onset voltage of negative corona on stranded conductors", M. Sc. Thesis, Faculty of Engineering, Banha University, 2007.
12. M. Abdel-Salam and E. K. Stanek, " On the calculation of breakdown voltages for uniform electric fields in compressed air and SF₆" , IEEE Transactions on Industrial Applications, Vol. 24, No. 6 November/December 1988.
13. N. H. Malik, " A review of the charge simulation method and its applications", IEEE Transactions on Electrical Insulation, Vol. 24, No.1, pp. 3-14, February, 1989.
14. K.S. Lyer and K.P.P. Pillai, "Analysis of irregularity factor of stranded conductors", Proc. IEE, Vol. 115, pp. 364-367, 1968.
15. G. E. Adams, "Voltage gradients on high voltage transmission lines", AIEE Transactions, Vol. 74, Pt. III, pp. 5-11, 1955.
16. A. Pederson, " The effect of surface roughness on breakdown in SF₆", IEEE Transactions on Power Apparatus and Systems, Vol. PAS-94, No, 5, pp. 1749-1754, 1975.

Appendix A: Potential and Electric field calculation [4,11]

A1. Transformation of Co-ordinates

The number of simulating finite line charges in each pitch equals $N [= n \times (3 n_o + n_g)]$, however, only the unknown simulating charges are those in pitch-0 because the pitches are repeated. Each finite line charge will be assigned to a Cartesian co-ordinate system (x_j, y_j, z_j) . By transformation of co-ordinates, an arbitrary point $A_i(x, y, z)$ is referred to these new coordinates. A coordinate transformation will be conducted for the complete arrangement of simulation line charges.

A2. Potential Calculation

The potential ϕ_i at an arbitrary contour point $A_i(x, y, z)$, due to the simulation line charges Q_j , ($Q_j = q_{j,0}, j = 1, 2, \dots, N$), is calculated by the relation

$$\phi_i = \sum_{j=1}^{j=N} P_{i,j} Q_j \quad (\text{A1})$$

where, $P_{i,j}$ is the summation of potential coefficients $p_{i,j,k}$ at the point $A_i(x, y, z)$ due to all simulation line charges,

$$P_{i,j} = \sum_{k=-\infty}^{k=\infty} p_{i,j,k} \tag{A2}$$

where, the potential coefficient $p_{i,j,k}$ is expressed as

$$p_{i,j,k} = \frac{1}{4\pi\epsilon l_j} \ln \left(\frac{[(1_j - x_{1j}) + \gamma_{1j}]}{[(-x_{1j}) + \delta_{1j}]} \right) \tag{A3}$$

where, l_j is the length of finite line charge,

$$\gamma_{1j} = \sqrt{(1_j - x_{1j})^2 + y_{1j}^2 + z_{1j}^2} \quad \text{and} \quad \delta_{1j} = \sqrt{x_{1j}^2 + y_{1j}^2 + z_{1j}^2}$$

Equating the applied voltage with the calculated potential at the selected boundary points results in a set of equations whose solution determine the unknown simulation charges.

A3. Electric Field Calculation

The differentiation of potential ϕ_i in the coordinate system (x_l, y_l, z_l) is conducted separately. Thus the components of the electric field, $(E_{xli,j}, E_{yli,j}$ and $E_{zli,j})$, of charge Q_j in the co-ordinate system (x_l, y_l, z_l) are obtained. These components must be transformed back and added into the main co-ordinate system (x, y, z) . Hence, for each finite line charge Q_j at a contour point $A_i(x, y, z)$, the field intensity components $E_{xi,j}$, $E_{yi,j}$ and $E_{zi,j}$ are

$$\begin{aligned} E_{xi,j} &= E_{xli,j} \cos \delta_j \cos \beta_j - E_{yli,j} \sin \beta_j - E_{zli,j} \sin \delta_j \cos \beta_j \\ E_{yi,j} &= E_{xli,j} \cos \delta_j \sin \beta_j + E_{yli,j} \cos \beta_j - E_{zli,j} \sin \delta_j \sin \beta_j \\ E_{zi,j} &= E_{xli,j} \sin \delta_j + E_{zli,j} \cos \delta_j \end{aligned} \tag{A4}$$

where, the angles δ_j and β_j are the inclination angles of a line charge on x-y and x-z planes, respectively. Then, the field intensity components E_{xi} , E_{yi} , and E_{zi} at point $A_i(x, y, z)$ due to all simulation line charges are obtained. Hence, the field intensity at that point is calculated by the relation

$$E_i = \sqrt{E_{xi}^2 + E_{yi}^2 + E_{zi}^2} \tag{A5}$$

المجالات ومعاملات تعرج السطح للموصلات المجدولة التي تمتد على محور أسطوانة

في هذا البحث تم حساب المجالات الكهربائية بالقرب من الموصلات المجدولة التي تمتد على محور أسطوانة وذلك باستخدام طريقة تمثيل الشحنات، و تم تمثيل الموصل و الأسطوانة بشحنات لولبية وحساب المجال الكهربى فى هذه الثغرة فى الأبعاد الثلاثة ، وكانت نتيجة تمثيل الشحنات دقيقة لدرجة أن نسبة الخطأ فى حساب الجهد وزاوية إنحراف المجال على سطح الموصل لم يتعدى % 0.1 ، 3.2 درجة على التتابع وذلك للموصلات 7, 19, 37 المجدولة ذات الأقطار 2 مم , 50 مم , ووجد أن حساب المجال على سطح هذه الموصلات ذات نفس القطر تقريبا متساوى ولا يعتمد على عدد الأسلاك فى الموصل المجدول (يساوي تقريبا 1.4 من قيمة المجال على سطح الموصل الأسطوانى الأملس)، بينما يختلف المجال الكهربى لهذه الموصلات بالقرب من سطح الموصل ، وتم أيضا حساب معامل التعرج للموصلات المجدولة المعزولة بالهواء ومقارنتها بالنتائج العملية والنظرية المدونة بالأبحاث المنشورة سابقا وتطابقت معها إلى حد كبير، و تم دراسة تأثير تغيير قطر الموصل على قيمة معامل التعرج للموصلات المجدولة والمعزولة بالهواء أو غاز سادس فلوريد الكبريت ووجد أن هذا المعامل ينخفض بزيادة القطر كما أنه ينخفض أكثر فى حالة العزل بغاز سادس فلوريد الكبريت ، و تم أيضا دراسة تأثير زيادة ضغط الهواء وغاز سادس فلوريد الكبريت على معامل التعرج ووجد أن هذا المعامل ينخفض بزيادة ضغط الغاز، ونظرا لأن غاز سادس فلوريد الكبريت غير مرغوب فيه بيئيا تم حساب ضغط الهواء المناظر فى شدة عزله لضغط غاز سادس فلوريد الكبريت.